Journal of Nano- and Electronic Physics
Vol. **9** No 5, 05033(5pp) (2017)

Журнал нано- та електронної фізики
Том **9** № 5, 05033(5cc) (2017)

Optical Phenomena and Processes Induced by Ultrashort Light Pulses in Chalcogenide and Chalcohalide Glassy Semiconductors

I. Blonskyi[1], V. Kadan[1], A. Rybak[1], S. Pavlova[1], L. Calvez[2], B. Mytsyk[3], O. Shpotyk[4,5]

[1] *Institute of Physics of the NAS of Ukraine, 46, NaukyProsp., 03680 Kyiv, Ukraine*
[2] *UMR-CNRS 6226, Université de Rennes 1, 35042 Rennes Cedex, France*
[3] *Karpenko Physico-Mechanical Institute of the NAS of Ukraine, 5, Naukova Str., 79060 Lviv, Ukraine*
[4] *Vlokh Institute of Physical Optics, 23, Dragomanov Str., 79005 Lviv, Ukraine*
[5] *Institute of Physics of Jan Dlugosz University, 13/15, al. Armii Krajowej, 42200 Czestochowa, Poland*

(Received 31 August 2017; published online 16 October 2017)

Time-resolved microscopy study of ablation with femtosecond laser pulses in chalcohalide glass and crystal silicon is presented. The laser pulse energy is deposited into the near-surface layer due to two-photon absorption. The superheated liquid is ejected from the ablation spot under the action of supersonic blast wave. Glass-forming process in chalcohalide glass creates optically smooth spherical surface of the crater due to the action of surface tension forces. As a result, single laser pulse produces microlens, which can be transformed into micromirrors after metal sputtering. The fabricated microoptical elements demonstrate diffraction-limited performance.

Keywords: Femtosecond laser pulses, Ablation, Chalcohalide glasses, Time-resolved microscopy.

DOI: 10.21272/jnep.9(5).05033 PACS numbers: 42.65.Re, 42.65.Jx, 52.38.Dx

1. INTRODUCTION

Laser processing of optical materials, particularly IR transparent crystal silicon (c-Si) and chalcohalide glasses (ChHG) offer significant advantages over more traditional photolithography, such as high speed, flexibility to produce custom devices, low cost. Special properties of femtosecond (fs) laser pulses, such as high strength of the E/M field, which is close to the ionization threshold of the medium, ultrashort pulse duration τ_p, comparable to the shortest characteristic times of the nonlinear response of the medium, make them an attractive instrument of laser micromachining. Fs laser damage features inhibition of thermal conductivity, i.e. heat affected zone becomes comparable to the length of light absorption. Therefore, in combination with largely non-thermal mechanism of the fs laser ablation, the surface of the machined material remains almost non-modified thermally. As a result, opaque materials can be process with very high quality. On the other hand, high intensity of the E/M field of the fs laser pulses generates plasma due to multiphoton absorption and controllable development of the avalanche breakdown in the focal spot inside transparent materials. This allows fabrication of microoptical elements in the bulk of transparent material, modifying its refractive index due to the local deposition of precise portions of light energy. Moreover, surface ablation of transparent IR materials also becomes possible at sufficiently high level of the light intensity on the surface.

The use of the fs lasers is complicated by the fact that new phenomena arise in the conditions of extreme temporal and spatial localization of the E/M field: generation of filaments, spatio-temporal transformation of the pulse propagating in nonlinear medium, widening of the pulse spectral band as a result of the self-phase modulation. These phenomena should be taken into account when using fs lasers as a micromachining instrument

Recent progress of optoelectronics has necessitated the development of microoptical elements, i.e. small-sized (< 1 mm) devices for light control. Transmissive and reflective optical elements, such as microlenses and micromirrors and their arrays are now important constituents of microoptics. Wide spectral range and absence of chromatic aberrations make micromirrors most suitable as components of microspectral devices for medicine and microbiology. Multiple optical tweezers, based on the ability of micromirror arrays to produce arrays of bright light spots, can be integrated into various lab-on-a-chip microfluidic analytic systems. They trap micro-particles, particularly biological cells, in focal spot area, increasing thereby the speed and performance of the relevant studies [1]. Microlaser resonators can be built using concave micromirrors [2], making them an important constituent of adaptive optics, telecom systems and matrix laser displays [3].

Several methods have been reported for fabrication of concave micromirrors, including the use of molds with concave spherical microlens arrays [1], photolithography [4], maskless lithography based on digital micromirror device [5], photolithography followed by ion implantation and electrochemical anodization [6].

Due to wide transparency ranging from mid- to far-IR [7], good mechanical and chemical stability, silicon and chalcohalide glasses attract close attention of investigators as materials for IR optoelectronics and telecommunications. To the best of our knowledge, only one group reported direct fabrication of microlens arrays in organic compounds using a single fs laser pulse for each lens, these being concave arrays in polydimethylsiloxane (PDMS) [8] and convex lens arrays in polymethylmethacrylate (PMMA) [9]. Since PDMS and PMMA are IR-opaque, highly productive single-step fabrication technology of microlenses and micromirrors in IR-transparent glassy materials is still required. Moreover, there are no data in the literature on the micromirror fabrication using single-pulse fs laser

ablation process.

This work is focused on physical phenomena induced by femtosecond laser pulses with the central wavelengths of 800 nm in crystalline silicon (c-Si) and chalcohalide (ChHG) glassy semiconductors. We describe a rapid process of direct single-pulse fabrication of microlenses and micromirrors developed for ChHG. Since various fabrication techniques of embedded waveguides in glassy media have previously been developed [10, 11], this process opens the way to fabricate complex integrated 3D micro-optics.

2. EXPERIMENTAL

The fabrication procedure of ChHG specimen is reported elsewhere [12]. The procedure follows the conventional melt-quenching route. It uses the purified ingredients: 65% GeS_2, 25% Ga_2S_3, and 10% CsCl, sealed in a vacuumized silica ampoule at 10^{-4} Pa. After several hours in a rocking furnace at 850°C and quenching in water at room temperature, a cubic sample (5×5×5 mm) with flat polished surfaces have been made from the resulting material. The residual mechanical stresses have been removed by annealing the sample at 395 °C for 4 h. The sample demonstrates a wide transparency window (0.5 ÷ 11 μm) inherent to this glass composition [12].

The single-pulse laser ablation was carried out in c-Si and ChHG samples S according the scheme shown (Fig. 1a).

Temporal dynamics of the femtosecond ablation in c-Si and glassy semiconductors has been studied using time-resolved pump-probe microscopy setup, which is schematically shown in Fig. 2a.

3. RESULTS AND DISCUSSION

The single-pulse laser ablation was carried out in c-Si and ChHG samples S with laser pulses of different energy E_p varying from 5 to 30 μJ at different positions $\delta = (\pm 400$ μm) of the focal plane of the lens L relative to the surface of the sample S (Fig.1a). Specific pulse energy was set by rotating the polarization plane of the laser beam with a $\lambda/2$ retardation plate placed before the Glan prism G. Apart from the angular position of the crystal axis of the $\lambda 2$ plate, the pulse total energy and energy distribution at the focal spot of the lens L (3.7×, 0.11 NA, $F = 3.4$ cm), (so called Airy pattern, which is formed as a result of diffraction on the aperture A [17]) depend on the diameter D of the aperture A (varied from 1 to 3 mm) before the lens L. The radial intensity distribution $I(r)$ in the Airy pattern is described by the square of the Bessel function of the first kind J_1 as $I(r) = (2J_1(x)/x)^2$,where $x = \pi r D/\lambda F$ with D as the aperture diameter, λ – wavelength, and $F =$ 3.4 cm – focal distance of the lens. The central part of the distribution $I(r)$ between the first zeros of the Bessel function contains ~ 95% of the total energy of the pulse.

After ablation the samples were examined using optical- and scanning electron microscopy (SEM). In Fig. 1 the pictures of the ablated area for ChHG and c-Si, taken with optical microscopy (Fig. 1b, d, e) and SEM (Fig. 1c) are compared. Microscopic inspection reveals that ablation in c-Si does not leave craters with smooth surface (Fig. 1d, e). The pulse with $E_p = 12$ μJ only modifies the surface of c-Si (Fig. 1d), while at $E_p = 25$ μJ rough ablation crater remains, surrounded by a ring-shaped modified area (Fig. 1e). We suppose that both the modified area and the surface of ablation crater consist of amorphous silicon. Indeed, the authors of [13] using cross-sectional transmission electron microscopy and energy dispersive x-ray analysis showed that in similar conditions an amorphous Si layer is formed in a zone adjacent to the ablated holes in c-Si. They explain formation of the amorphous layer in such a way that a molten zone surrounding the ablated hole solidifies so rapidly that crystallization is bypassed.

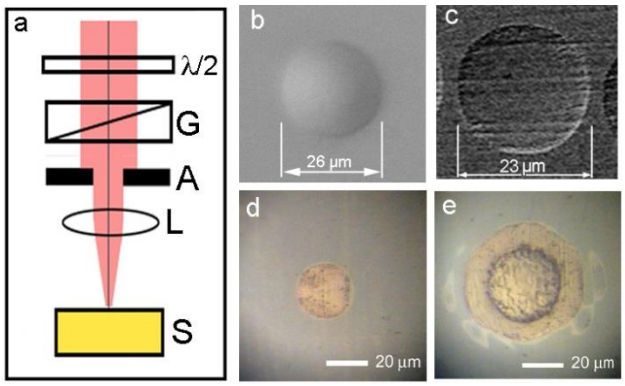

Fig. 1 – Outline of the ablation experiment (a); Modified area on the surface of ChHG at the pulse energy 12 μJ (b, c); Modified area on the surface of c-Si at the pulse of energy 12 μJ (d) and 25 μJ (e)

In contrast, both optical and SEM microscopy demonstrate predominantly smooth surface of the ablation craters in ChHG (Fig. 1 b, c). Moreover, microscopic inspection through the polished lateral face of the sample did not reveal any bulk damage or refractive index change beneath the surface of the ablated area. Thus, we conclude that no bulk damage is produced beneath the surface with the remaining energy fraction of the single fs pulse, which passed in depth of the sample after the surface absorption. Assuming the TPA coefficient for $As_4Ge_{30}S_{66}$ ChHG with the similar band gap $\beta = 8 \times 10^{-10}$ cm/W [15] as an estimate, we obtain, that the initial pulse energy decreases 2.7 times on the depth of 0.85 μm due to TPA at the pulse energy 12 μJ, duration $\tau_p = 200$ fs, and the focal spot diameter 32.4 μm. So, considering small linear absorption in GeS_2-Ga_2S_3-CsCl ChHG at 800 nm [14], we believe that only nonlinear absorption (TPA+ inverse bremsstrahlung in laser-induced plasma) provides the laser energy deposition, needed for the ablation.

Next, we focus on temporal dynamics of the femtosecond ablation in c-Si and ChHG, studied using the time-resolved pump-probe microscopy setup, shown in Fig. 2a, in order to find physical mechanisms underlying the formation of the crater surface in both materials. The time-resolved microscopy setup has been created basing on the principal scheme reported earlier [16]. The sample S was ablated with a single pump pulse of ~ 150 fs duration with 800 nm wavelength, incident normally to the sample surface. To avoid the

scattered pump light, which hinders the registration, the temporal stages of the ablation process have been recorded using frequency-doubled pulse of the same laser at 400 nm wavelength, which was delayed for a certain variable time period τ_d in respect to the pump pulse. Changing τ_d with the optical delay line, not shown in the figure, we record different stages of the ablation process as transmission snap-shots of the probe beam, reflected from the sample S surface under a small angle of 13 °. In distinct from the other similar microscopy setups [17, 18], both the shape of the ablation spot itself and development of the blast wave above the spot can be recorded simultaneously in this scheme. Having taken a picture, we change τ_d and shift the sample to expose a new non-damaged place.

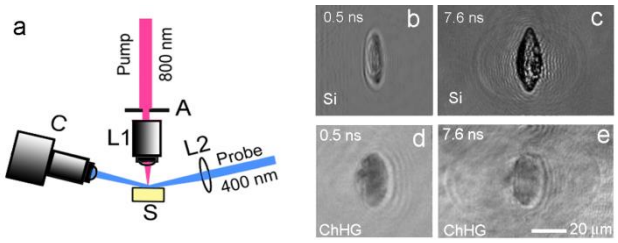

Fig. 2 – Femtosecond ablation dynamics in c-Si and ChHG. Combined transient transmission/reflection time-resolved microscopy setup (a). Stages of the fs laser ablation of c-Si (b, c) (E_p = 25 μJ) and ChHG (d, e) (E_p = 15 μJ) at different time delays τ, indicated on the upper left. The scale is the same for all pictures

Fig. 2b-e show several pictures of transient ablation stages in c-Si and ChHG taken at different time delays, which are indicated in their upper left side. At $\tau_d > 0$ increasing darkening appears at the ablation spot in ChHG. Transversal expansion of the ablation spot starts from $\tau_d \sim 130$ ps indicating the onset of material ejection from the excited area (Fig. 1d). Apart from the ejection of the material, blast wave of expanding plasma detaching from the ablation spot is formed at $\tau_d > 1.7$ ns (Fig. 2e). The blast wave front becomes visible due to the refraction of the probe beam on the abrupt change of the refractive index at the interface ablation species/air. Aspherical front of the blast wave expands supersonically, its maximum velocity υ_b being 9.7 km/s. We suppose that the toroidal formation seen on the crater edges at $\tau_d \sim 1.7$-7.6 ns (Fig. 2e) is formed by the molten material expulsed from the ablation spot by the pressure of the blast wave. However, no marked rim remains after solidification (Fig. 1b, c). We believe that this is the result of the subsequent evaporation of the overheated liquid material. The fs laser ablation in borosilicate glass [19] and in PDMS [8] also results in clean surface of the ablation craters. This has been explained as a result of expulsion of the liquid material by the pressure force of the blast wave and its smoothening by the forces of surface tension before solidification. We believe that similar mechanisms are responsible for the formation of the crater surface also in our case.

In c-Si femtosecond laser ablation occurs largely according to the same scenario (Fig. 2b, c). However, the expansion velocity of the blast wave front υ_b = 7 km/s is smaller in c-Si, and, as we have already reported above, rough crater surface covered with the amorphized layer is created. The depth of linear absorption in c-Si is 10 μm at 800 nm. However, estimation shows, that the initial pulse energy decreases 2.7 times on the depth of 0.8 μm due to TPA at the pulse energy 25 μJ, duration τ_p = 200 fs, and the laser spot diameter 32.4 μm Here, we use the TPA coefficient for c-Si $\beta = 4 \times 10^{-10}$ cm/W [20]. So, similar to the ChHG, the absorption length in c-Si is dominated by TPA, despite the relatively small length of linear absorption. Smaller propagation velocity of the blast wave front υ_b = 7 km/s could be explained by a significantly higher melting point of the crystalline silicon 1414 °C, twice as high as that of ChHG. However, substantially different conditions of solidification, such as surface amorphization and recrystallization in c-Si and glass formation in ChHG, result in different surface quality of ablation crater.

As the next step, in order to fabricate micromirrors, we covered the ablated surface of ChHG with a 20 nm-thick gold layer by vacuum deposition. Among all metals, gold coating is the best choice, providing the best IR reflectivity, which exceeds 99 % for the 0.7-20 μm range. Thus, spherical concave micromirrors have been formed. In distinct from diverging concave microlenses, they form real focus with focal distance approximately twice as short as that of microlenses. Accordingly, their NA is twice as large as that of microlenses.

Next we turn to the comparative characterization of the fabricated microlenses and micromirrors. The results of characterization for the microlenses has been reported by us earlier in [21]. Fig. 3a shows the virtual focal spot formed by the concave microlens with the radius of the spherical surface 159 μm, focal distance – 142 μm and numerical aperture – NA = 0.09. The picture was obtained under illumination with red LED (λ = 0.63 μm). The focal spot has diameter d = 7.7 μm between the first zeros of the Airy pattern, which demonstrates diffraction-limited performance of the lens. After gold plating of the same microlens, concave micromirror was produced with the real focal distance 80 μm and NA = 0.15. Fig. 3d shows the focal spot of this micromirror under red LED illumination with λ = 0.63 μm. Diameter of the focal spot d = 5.0 μm between the first zeros of the Airy pattern also proves diffraction-limited performance of the micromirror.

Apart from the focal spots, we compare real image of the letters IΦ (abbreviation of Institute of Physics in Ukrainian) formed by the micromirror (Fig. 3b) and virtual image of the letters IP (Institute of Physics) formed by the original microlens with the radius of surface curvature 159 μm (Fig. 3e). The configurations of the measurements are schematically shown in Fig. 3c for the micromirror, and in Fig. 3f for the microlens. Care has been taken in the case of micromirror measurement to form collimated illuminating beam coming out from the microscopic lens (Fig. 3c). Letters IP have been printed on white paper, and the letters IΦ – on transparency. It is obvious from the Fig. 3b, e, that similar to the focal spots, the micromirror provides better imaging resolution about 2 μm.

Apart from single microlenses, we also formed microlens array, scanning the ChHG surface with repetitive laser pulses at 100 Hz repetition rate. Thus, we covered the area 1 × 1 mm with identical concave micro-

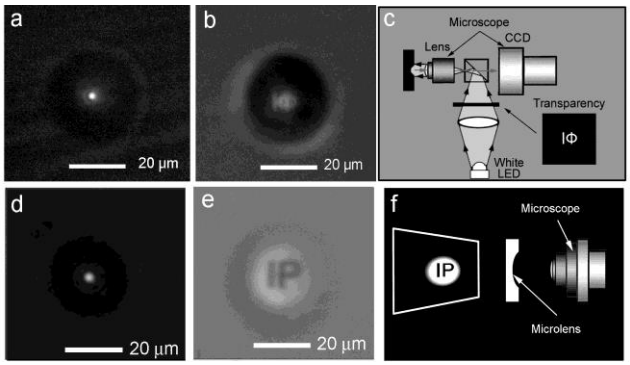

Fig. 3 – Focal spot of the micromirror (a). Real image formed by the micromirror (b). Registration scheme of the image, formed by the micromirror (c). Focal spot of the microlens (d). Virtual image formed by the microlens (e). Registration scheme of the image, formed by the microlens (f)

lenses of 17 μm diameter and 100 μm focal distance each. After that we coated the obtained microlens array with gold to produce array of micromirrors. Optical microscopy picture of the original microlens array is presented in Fig. 4a. Fig. 4b shows array of virtual foci, formed by these microlenses, and array of real foci, formed by micromirrors (Fig. 4c). Comparison of the Fig. 4b and Fig. 4c demonstrates, that again, similarly to single microlens and micromirror (Fig. 3a, d), the micromirrors form the array of smaller focal spots, than that of the microlenses.

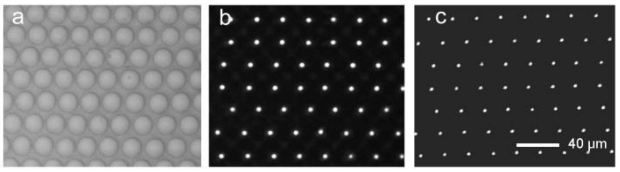

Fig. 4. – Microlens array (a). Array of virtual foci (b). Array of real foci (c)

Note, that any required configuration of the array can be produced very rapidly just changing control code, providing the synchronization of pulse sequence with positioning of the 2D-stage is performed. In that case the performance of the process will be limited only by the pulse repetition rate and positioning speed.

4. CONCLUSIONS

In conclusion, temporal stages of ablation of c-Si and ChHG with single fs laser pulses with wavelength 800 nm has been studied using time-resolved microscopy. We showed that transfer of the laser pulse energy to the sub-micrometer near-surface layer of the material occurs manly due to TPA both in c-Si and ChHG. Ejection of the superheated liquid material from the ablation crater is assisted by the high pressure of supersonic blast wave, propagating with maximum velocity 7 km/s in c-Si and 9.7 km/s in ChHG. In c-Si, amorphization and recrystallization occurring in the process of solidification result in poor optical quality of the surface of ablation crater. In ChHG after solidification, the surface of the ablation crater acquires optically smooth spherical surface due to the action of the forces of surface tension in the glass-forming process. Using the single-pulse ablation, we formed microlenses and microlens arrays in ChHG. Micromirrors and micromirror arrays were produced by coating the ChHG microlenses with 20 nm-thick gold layer. Both microlenses and micromirrors demonstrate diffraction-limited performance. To the best of our knowledge, this is the first use of single-pulse ablation process for fabrication of microlenses and micromirrors in glassy media. Rapid production technology of arbitrarily complex microlens- and micromirror arrays can be developed basing on the above process.

ACKNOWLEDGEMENTS

The authors acknowledge support from the STCU-NASU (project 6174), NASU-TÜBİTAK (joint project), as well as from the Ukrainian State Fund for Fundamental Research (Project F73/23805).

Оптичні явища і процеси, індуковані ультракороткими лазерними імпульсами в халькогенідних та халькогалоїдних склоподібних напівпровідниках

І. Блонський[1], В. Кадан[1], А. Рибак[1], С. Павлова[1], Л. Кальвез[2], Б. Мицик[3], О. Шпотюк[4,5]

[1] *Інститут фізики НАН України, проспект Науки 46, 03680 Київ, Україна*
[2] *UMR-CNRS 6226, Університет Рен 1, 35042 Рен CEDEX, Франція*
[3] *Фізико-механічний інститут ім. Карпенка НАН України, вул. Наукова, 5, 79060, Львів, Україна*
[4] *Інститут фізичної оптики ім. О.Г. Влоха, вул. Драгоманова. 23, 79005 Львів, Україна*
[5] *Інститут фізики Університету Яна Длугоша, ал. Армії Крайовей 13/15, 42200 Ченстохова, Польща*

У роботі представлені результати вивчення абляції халькогалоїдного скла і кристалічного кремнію фемтосекундними лазерними імпульсами з використанням часороздільної мікроскопії. Енергія лазерного імпульсу передається у приповерхневий шар через двохфотонне поглинання. Перегріта рідина витискається з зони абляції під дією надзвукової ударної хвилі. В процесі охолодження і утворення скла поверхня кратера в халькогалоїдному склі розгладжується під дією сил поверхневого натягу. Таким чином, єдиний лазерний імпульс створює мікролінзу, з якої можна створити мікродзеркало шляхом нанесення металевого покриття. Створені мікрооптичні елементи є дифракційно обмеженими.

Ключові слова: Фемтосекундні лазерні імпульси, Абляція, Халькогалоїдне скло, Часороздільна мікроскопія.

Оптические явления и процессы, индуцированные ультракороткими лазерными импульсами в халькогенидных и халькогалоидных стеклообразных полупроводниках

И. Блонский[1], В. Кадан[1], А. Рыбак[1], С. Павлова[1], Л. Кальвез[2], Б. Мыцык[3], О. Шпотюк[4,5]

[1] *Институт физики НАН Украины, Проспект Науки 46, 03680 Киев, Украина;*
[2] *UMR-CNRS 6226, Университет Рен 1, 35042 Рен CEDEX, Франция;*
[3] *Физико-механический институт им. Карпенко НАН Украины, ул. Наукова 5, 79060 Львов, Украина*
[4] *Институт физической оптики им. О.Г. Влоха, ул. Драгоманова. 23, 79005 Львов, Украина;*
[5] *Институт физики Университета Яна Длугоша, ал. Армии Краёвей 13/15, 42200 Ченстохова, Польша*

В работе представлены результаты изучения абляции халькогалоидного стекла и кремния фемтосекундными лазерными импульсами с использованием микроскопии с разрешением по времени. Энергия лазерного импульса передается в приповерхностный слой путем двухфотонного поглощения. Перегретая жидкость вытесняется из зоны абляции под действием сверхзвуковой ударной волны. В процессе охлаждения и образования стекла поверхность кратера в халькогалоидном стекле разглаживается под действием сил поверхностного натяжения. Таким образом, единственный лазерный импульс создает микролинзу, из которой можно создать микрозеркало путем нанесения металлического покрытия. Созданные микрооптические элементы являются дифракционно ограниченными.

Ключевые слова: Фемтосекундные лазерные импульсы, Абляция, Халькогалоидное стекло, Мікроскопія с временным разрешением.

REFERENCES

1. F. Merenda, J. Rohner, J-M. Fournier, R. Salathe, *Opt. Express* **15**, 6075 (2007).
2. R. Aldaz, M. Wiemer, D. Miller, H. James Jr., *Opt. Express* **12**, 3967 (2004).
3. H. Zappe, *Fundamentals of Micro-Optics* (Cambridge: Cambridge University Press: 2010).
4. Y. Awatsuji, M. Sasada, N. Kawano, T. Kubota, *Jpn. J. Appl. Phys.* **43**, 5845 (2004).
5. Z. Zhang, Y. Gao, N. Luo, K. Zhong, *AIP Advances* **6**, 015319 (2016).
6. Y.S. Ow, M. Breese, S. Azimi, *Opt. Express* **18**, 14511 (2010).
7. J-L. Adam, X. Zhang, *Chalcogenide Glasses: Preparation, Properties and Applications* (Philadelphia-New Delhi: Woodhead Publ. Ser. in Electron. and Opt. Mat.: 2013).
8. J. Yong, F. Chen, Q. Yang, G. Du, H. Bian, D. Zhang, J. Si, F. Yun, X. Hou, *ACS Appl. Mater. Interfaces* **5**, 9382 (2013).
9. Y. Ou, Q. Yang, F. Chen, Z. Deng, G. Du, J. Wang, H. Bian, J. Yong, X. Hou, *IEEE Photonics Tech. Lett.* **27**, 2253 (2015).
10. I. Blonskyi, V. Kadan, O. Shpotyuk, M. Iovu, P. Korenyuk, I. Dmitruk, *Appl. Phys. B* **104**, 951 (2011).
11. P. Masselin, D. Le Coq, E. Bychkov, E. Lépine, C. Lin, L. Calvez, *Proc. SPIE* **7993**, 79931B (2011).
12. Y. Ledemi, L. Calvez, M. Roze, X.H. Zhang, B. Bureau, M. Poulain, Y. Messaddeq, *J. Optoelectron. Adv. Mater.* **9**, 3751 (2007).
13. J. Jia, M. Li, C.V. Thompson, *Appl. Phys. Lett.* **84**, 3205 (2004).
14. C. Lin, L. Calvez, B. Bureau, Y. Ledemi, Y. Xu, H. Tao, X. Zhang, X. Zhao, *J. Optoelectron. Adv. Mater.* **12**, 1684 (2010).
15. I. Blonskyi, V. Kadan, O. Shpotyuk, M. Iovu, I. Pavlov, *Opt. Mater.* **32**, 1553 (2010).
16. I. Blonskyi, M. Brodyn, V. Kadan, O. Shpotyuk, I. Dmytruk, I. Pavlov, *Appl. Phys. B* **97**, 829 (2009).
17. K. Sokolowski-Tinten, J. Bialkowski, A. Cavalleri, D. von der Linde, A. Oparin, Meyer-ter-Vehn, S.I. Anisimov, *Phys. Rev. Lett.* **81**, 224 (1998).
18. K. Sokolowski-Tinten, J. Bialkowski, M. Boing, A. Cavalleri, D. von der Linde, *Phys. Rev. B* **58**, R11805 (1998).
19. A. Ben-Yakar, A. Harkin, J. Ashmore, R.L. Byer, H.A. Stone, *J. Phys. D: Appl. Phys.* **40**, 1447 (2007).
20. A.D. Bristow, N. Rotenberg, H.M. van Driel, *Appl. Phys. Lett.* **90**, 191104 (2007).
21. V. Kadan, I. Blonskyi, Y. Shynkarenko, Rybak, . Calvez, B. Mytsyk, O. Spotyuk, *Opt. Laser Technol.* **96**, 283 (2017).